

Lasers in Manufacturing Conference 2021

Influence of laser beam welding with overlaid high-frequency beam oscillation on weld seam quality and fatigue strength of aluminum wrought and die-cast joints

Benjamin Kessler^{a,*}, Dirk Dittrich^a, Robert Kuehne^a, Markus Wagner^a, Axel Jahn^a

^aFraunhofer Institute for Material and Beam Technology IWS, Dresden, Winterbergstraße 28, 01277 Dresden, Germany

Abstract

Laser beam welding of aluminum die cast components using high frequency beam oscillation could massively improve the process stability and tightness of cooling components. The application of the newly developed laser beam welding processes to fatigue loaded components makes it necessary for designers to dimension the components and welds using existing guidelines. Up to now, however, no experience has been obtained with the applicability of the existing regulations.

For this purpose within this study, weld specimens in form of aluminium mixed joints (wrought and die-cast alloys) were produced with standard laser beam welding process (LBW) and laser beam welding with overlaid high-frequency beam oscillation (LBW-HF). The weld seam quality is correlated with the fatigue strength properties. Furthermore, the results from the fatigue tests are classified in the existing IIW regulations and their applicability with regard to laser-welded aluminium joints will be discussed. The results show an increased fatigue strength, especially for the LBW-HF process, compared to current used standards for design.

Keywords: laser; laser beam welding; aluminum; beam oscillation; fatigue strength; high-frequency oscillation

1. Introduction and motivation

The use of aluminum alloys has been increasing constant since the 1980s. A main driver of this development is lightweight design efforts in various areas of transportation. Due to stricter legal requirements regarding carbon dioxide emissions and rising energy prices this development will move on the future. A major contribution to cost-effective mass production of aluminium components has been made by the die casting process (Winkler et al. 2004). Automobile manufacturers are therefore increasingly relying on a mixed construction of wrought and die-cast aluminium products, such as the vehicle manufacturer Audi for its A8 model (see Fig. 1).

* Corresponding author.

E-mail address: benjamin.kessler@iws.fraunhofer.de .

A disadvantage of the manufacturing route for die-cast material is that it results in components which have a limited weldability due to the gas content and inclusions resulting from the process. As a result, irregularities in the form of pores or blow outs occur during welding, which can reduce weld strength and would lead to a higher reject rate compared to wrought alloys. This can be overcome by innovative joining processes, such as laser beam welding with overlaid high-frequency laser beam oscillation or electron beam welding with multi-bath technology. These joining approaches addressing higher weld quality and would accordingly reduce rejects of the melt pool on die-cast materials (Dittrich et al. 2019, Börner et al. 2020 and Teichmann et al. 2017).

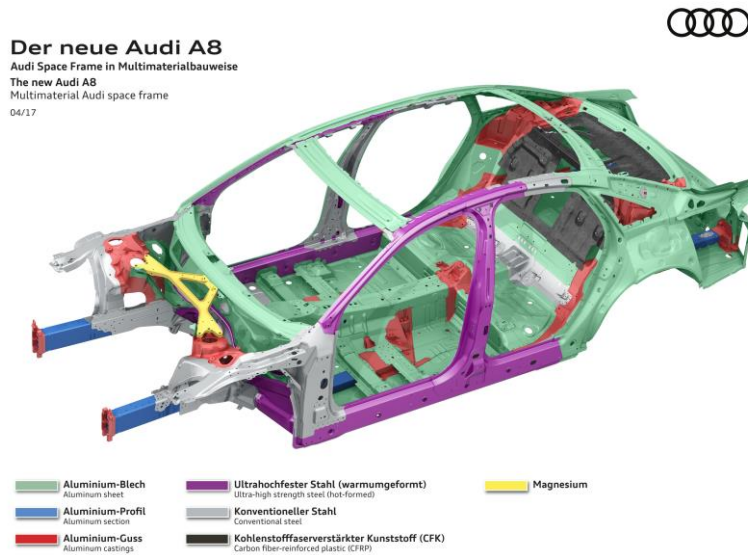


Fig. 1: Multimaterial space frame of the Audi A8 (© AUDI AG)

For this reason, the technology of laser beam welding of aluminium die casting provides a good opportunity for being used in production of serial components. Especially since the requirements in terms of static strength or tightness for media-carrying assemblies are given laser beam welding is considered. The focus of current research work is on understanding the process in order to further improve the weld seam quality. In the future it should also be possible to use laser welded components made of aluminium die castings that are subjected to cyclic loads. In addition to weld seam quality, one challenge is the dimensioning of such joints. Due to a lack of data, it has not yet been clarified whether the applicability of standardized design guidelines based on the nominal stress or notch stress concept is permissible.

The aim of this paper is to discuss this applicability by correlating data from fatigue tests and the FAT classes according to IIW recommendations and the notch stress concept according to DVS Code of Practice 0905. For this purpose, 3 different welded joints are produced from aluminium die casting and wrought alloys and their weld seam quality is determined by means of metallographic analyses.

2.1. Laser beam welding methods

Within the scope of this research, static laser beam welding and laser beam welding with high-frequency beam oscillation were investigated to compare seam quality.

The state of the art welding tests with static laser beam welding (LBW) were performed with a multimode fiber laser (IPG YLR 4000) and a focus diameter of $\sim 294 \mu\text{m}$. The welding tests with overlaid high-frequency beam oscillation (LBW-HF) were performed with a singlemode fiber laser (IPG YLS 5000 SM), the *remoweld*[®]FLEX welding optics and a galvanometer scanner (Scanlab GmbH weldDYNA[®]) and a focus diameter of $37 \mu\text{m}$. The oscillated laser beam followed equation 1. The frequency and amplitude ratio was 1 each, resulting in the oscillation figure of a circle. The amplitudes were 0.15 mm for all welding tests. Table 1 summarizes the optical characteristics of the components used.

$$\begin{pmatrix} x_{\text{Laser}}(t) \\ y_{\text{Laser}}(t) \end{pmatrix} = \begin{pmatrix} a_x \sin(2\pi f_x t + \Delta\varphi) \\ a_y \sin(2\pi f_y t + \Delta\varphi) \end{pmatrix} \quad (1)$$

The weld specimens were fixed during welding using a pneumatic clamping device. The weld metal was protected from oxidation on the upper side by means of argon 4.6. The root was not covered by shielding gas. Fig. 2 shows the experimental setup of both welding processes in the laser laboratory.

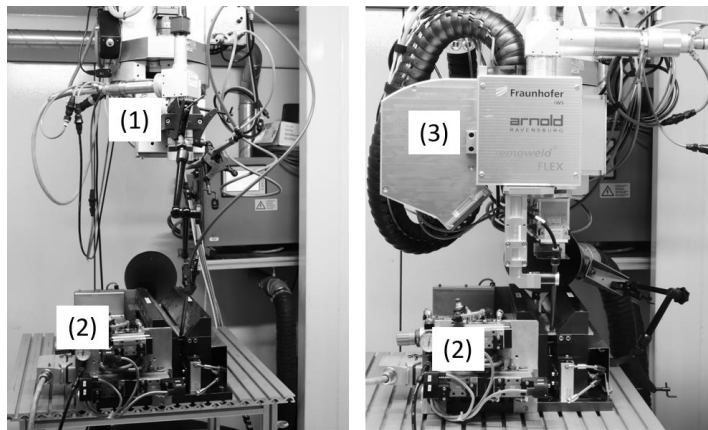


Fig. 2. left: welding set-up static LBW; right: LBW –HF; (1) welding optics, (2) clamping device, (3) remoweld[®]FLEX optics

Table 1. Overview of the optical components used

| | | LBW | LBW-HF |
|----------------------|---------------|--------------|-----------------|
| Laser beam source | - | IPG YLR 4000 | IPG YLS 5000-SM |
| Maximum laser power | kW | 4 | 5 |
| Beam quality | mm*mrad | 2 | 0,4 |
| Fiber diameter | μm | 50 | 30 |
| Focal diameter | mm | 294 | 37 |
| Galvanometer scanner | - | - | ja |

2.2. Materials and joint configuration

In the context of the results presented here, two die-casting alloys and a wrought alloy were investigated. The alloy AlSi9MnMoZr was available in the form of two casting charges. The objective was to determine if the casting batch had an effect on fatigue strength. In addition to the chemical composition (Table 2), the batches differ in their hydrogen contents. The hydrogen contents were analyzed by melt extraction (measuring instrument: Bruker G8 Galileo). It was found that batch one contains approx. 4.5 ppm hydrogen and batch two approx. 12.4 ppm hydrogen.

Table 2 summarizes the chemical compositions of the alloys used. The compositions were determined by spectral analysis.

Table 2. Average chemical composition in weight percentage of the used materials from 6 measurements

| | AlSi9MnMoZr (Charge 1) | AlSi9MnMoZr (Charge 2) | AlSi10MnMg | EN AW-6082 |
|----------------|------------------------|------------------------|--------------|------------|
| Si | 10,5-11,3* | 10,7-11,7*** | 11,3-12,4*** | 0,94 |
| Fe | 0,10 | 0,11 | 0,15 | 0,39 |
| Cu | 0,001 | 0,002 | 0,009 | 0,07 |
| Mn | 0,43 | 0,46 | 0,71 | 0,47 |
| Mg | 0,005 | 0,005 | 0,33 | 0,76 |
| Zn | 0,018 | 0,018 | 0,034 | 0,047 |
| Ti | 0,082 | 0,080 | 0,061 | 0,033 |
| Zr | 0,14 | 0,15 | 0,009 | < 0,005 |
| Mo | ** | ** | / | / |
| Al | 88,2 | 87,9 | 86,6 | 97,2 |
| H ₂ | 4,5 ppm | 12,4 | / | / |

* For the element silicon the smallest and the largest value of the 6 performed measurements were given.

** The element could not be analyzed with the device used.

The casting alloys were available in form of plates with the dimensions of 100 x 70 x 3 mm length x width x thickness. In the course of the welding tests, the plates were processed in 3 configurations by **butt welding** (see Table 3).

Table 3. Welding configurations investigated

| | Joining partner 1 | Joining partner 2 |
|-----------------|-----------------------|-----------------------|
| Configuration 1 | AlSi10MnMg | EN AW-6082 |
| Configuration 2 | AlSi9MnMoZr (Batch 1) | AlSi9MnMoZr (Batch 1) |
| Configuration 3 | AlSi9MnMoZr (Batch 2) | AlSi9MnMoZr (Batch 2) |

2.3. Fatigue tests and fatigue assessment using the notch stress concept

The fatigue strength was determined on a resonance test machine (Rumul Teststronic) with a test frequency of 88 Hz, a stress ratio of $R = 0.1$. The maximum number of load cycles was set to 2×10^6 . The test specimen geometry is shown in Fig. 3, left. The specimen where hydraulically clamped as shown in Fig. 3, right and fatigue tested up to failure. To prevent crack initiation at the edges of the specimen, they were work hardened.

The notch stress was determined in accordance with the recommendations of DVS Merkblatt 0905. The determined notch stresses are based on a linear-elastic material behavior and a fixed notch reference radius of $r = 0.05$ mm (plate thicknesses < 5 mm) was modeled in the notch root. The maximum element edge length in the finite element model was 0.008 mm in the notch base. The seam topographies were determined using a 3D microscope. The FE model was built two-dimensionally and symmetrically for a specimen length of 5 mm.

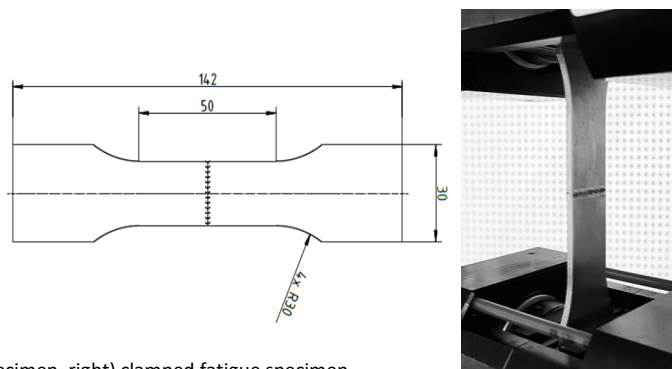


Fig. 3. Left) fatigue test specimen, right) clamped fatigue specimen

2. Results and Discussion

Fig. 5 shows the welding results in the form of metallographic cross sections. The development and application of both welding processes resulted in high-quality welds which, except for the porosity, correspond to weld quality class B according to DIN EN ISO 13919-2. The porosity observed in the cross-section during welding can be improved by the application of high-frequency laser beam oscillation in all 3 configurations compared to the static laser beam welding process. The assessment of the porosity of a characteristic longitudinal section of configuration 2 confirms and consolidates this observation. The pores are reduced in total by the beam oscillation to 2.3 % of the cross section area and their maximum size decreases to 230 μm for configuration 2. The higher hydrogen content of configuration 3 compared to 2 leads to higher pore formation in both welding processes. Furthermore, it was observed for all welding processes that the formation of the weld seam root is more uniform, i.e. more stable, when beam oscillation is used.

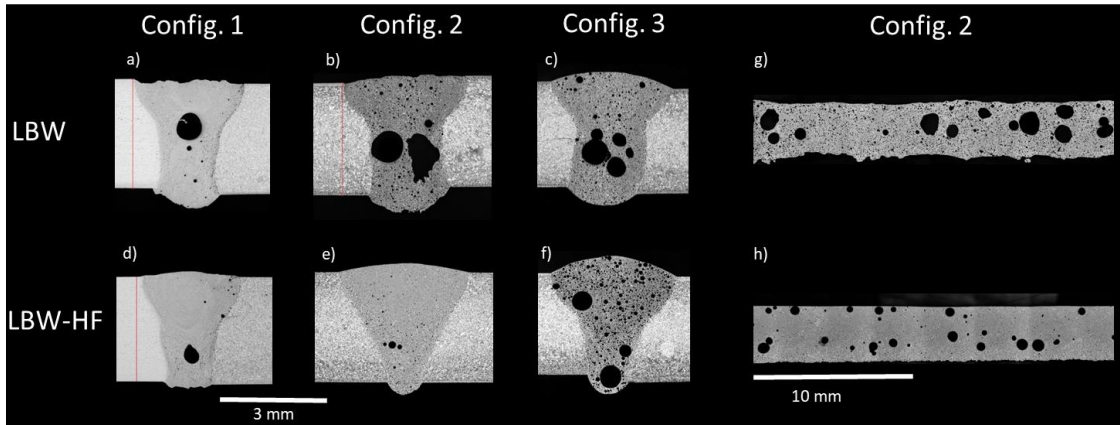


Fig. 4. a) LBW - configuration 1; b) LBW - configuration 2, c) LBW - configuration 3; d) LBW-HF - configuration 1; e) LBW-HF - configuration 2, f) LBW-HF - configuration 3, g) LBW - configuration 2, h) LBW-HF configuration 2

The results of the fatigue test in the form of the test specimens and the S-N-curves determined from the tests for a 97.7% survival probability, as well as the numbers of load cycles to failure determined from the notch stress concept, can be found in Fig. 6, 7 and 8. The S-N-curves determined from the tests are based only on the fractures in the weld (black and blue symbols). For illustration purposes, the tests without fracture (green symbols) and the tests with fracture in the base material (red symbols), which are due to internal material irregularities, are also entered in the diagrams. Basically, the results reflect that welded joints made of aluminum die casting are dependent on the base material quality. In particular, a large number of fractures in the base metal were observed in configurations 2 and 3 (cast-only joints). It is interesting to note that the load cycles to failure of the specimens with fracture in the base metal fall within the scatter band of the specimens with fracture in the weld.

The design of the welded joint according to the nominal stress concept can be done with FAT 12, 20 or 28 (see Fig. 5), depending on the test. In the following diagrams, FAT 28 was used because it represents the optimum. The FAT 28 entered in the diagrams (valid for the R=0.5) was converted by a factor of 1.16 for comparability for R=0.1 (Hobbacher A.F. et al. 2016).

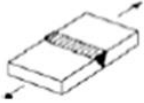
| No. | Structural Detail | Description (St. = steel; Al. = aluminium) | FAT St. | FAT Al. |
|-----|---|--|----------------|----------------|
| 216 |  | Transverse butt welds welded from one side without backing bar, full penetration Root checked by appropriate NDT including visual inspection NDT without visual inspection No NDT | 71 63 36 | 28 20 12 |

Fig. 5. IIW-recommendation for FAT class of the specific weld (Hobbacher A.F et al. 2016)

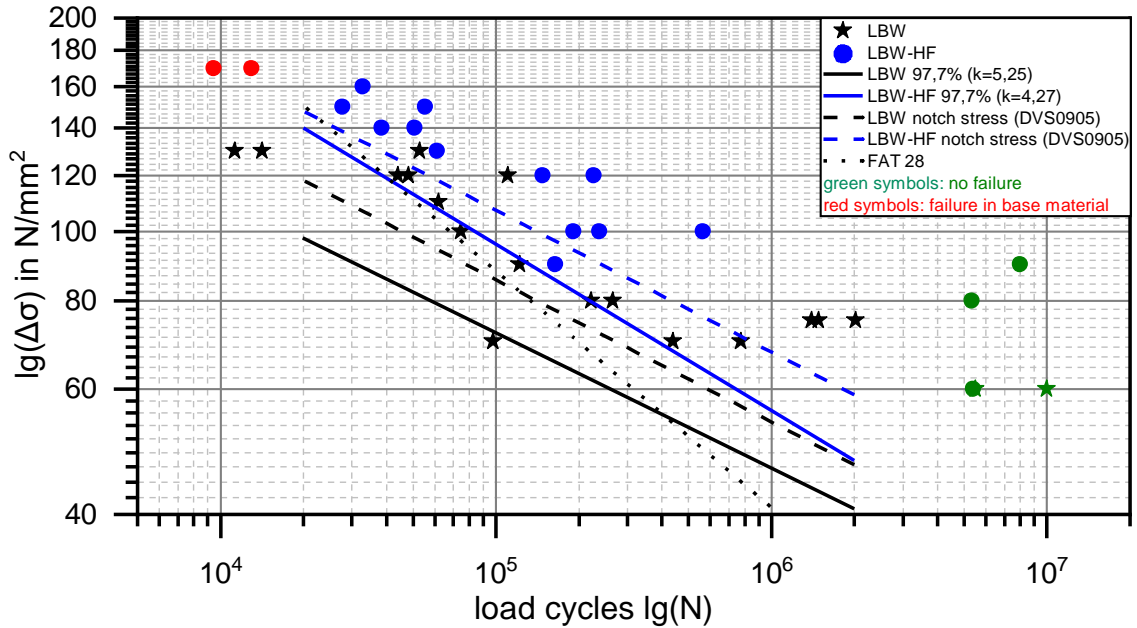


Fig. 6. Results of the fatigue tests of the configuration 1 (butt weld, 3 mm thickness, AlSi10MnMg vs. EN AW-6082)

The S-N-curves determined in the test show the following tendency for all 3 configurations:

- The tolerable load at $2E6$ load cycles is higher for the LBW-HF than the LBW specimens.
- Especially with increasing numbers of load cycles, the application of FAT 28 underestimates the strength of the welded joints. In relation to the FAT 28, the S-N-curves lie higher in the region of $2E6$ Load cycles.
- At high fatigue stress ($\Delta\sigma \geq 100 \text{ MPa}$) the determined life time of the test samples was lower than expected acc. to FAT28 Crack initiation occurs in weld specimens in the root region, which is a requirement to use the notch stress concept (see Fig. 8).
- Fractures in the base metal occur in case of LBW-HF at very high strength values. Fracture start at internal irregularities (see Fig. 8).

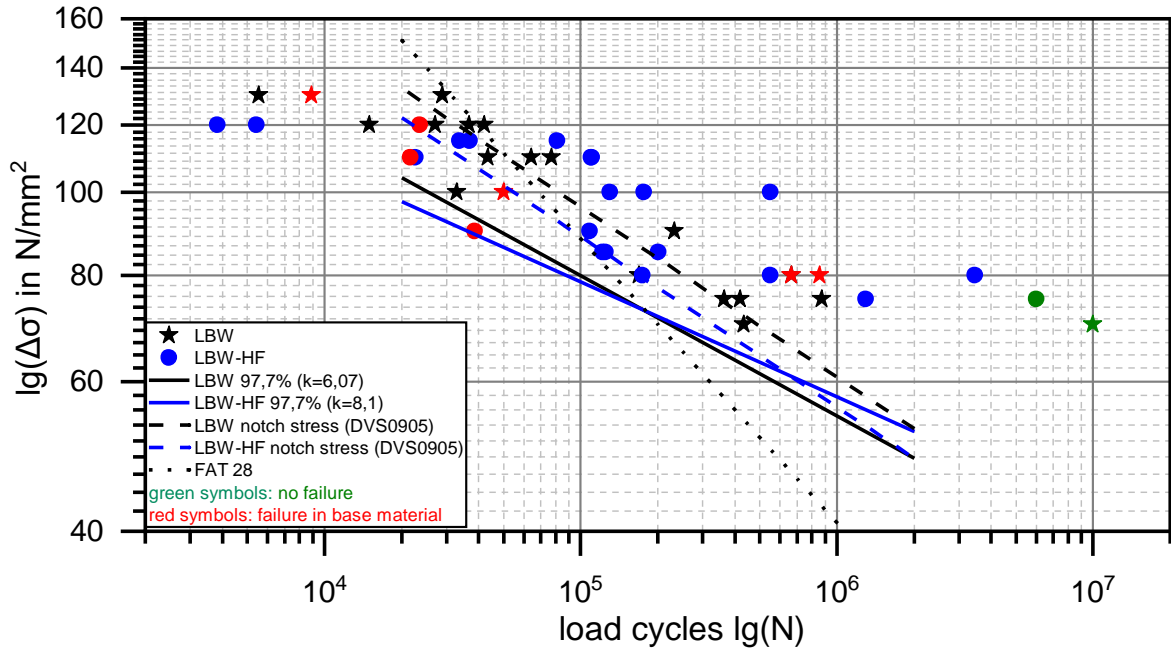


Fig. 7. Results of the fatigue tests of the configuration 2 (butt weld, 3 mm thickness, AlSi9MnMoZr (Batch 1) vs. AlSi9MnMoZr (Batch1))

The comparison of configurations 2 and 3 shows that batch 2 with increased hydrogen content exhibits more fractures in the base material on the one hand, and on the other hand that the strength and thus the number of cycles to failure are reduced for LBW. One assumption for the reason lies in the present nominal stress. This is probably higher due to the increased porosity in configuration 3. However, this is irrelevant for the design, as the designer must rely on a specific base material quality so that the number of pores in the base material and in the welds does not exceed a certain level. Therefore it is important to notice, that there is no influence on the fatigue strength of the batch by using the LBW-HF welding technology.

The application of the notch stress concept according to DVS 0905 provides a good approximation of the number of cycles to failure be at $2E6$ load cycles in all 3 configurations compared to the values determined in the test. Compared to the IIW recommendation (increase $k = 3$), the increase of $k = 5$ suggested in the specification comes closer to the values determined in the test ($k = 4.27 \dots 8.1$). In the area of the Wöhler line, the stress that can be derived from the notch stress concept is very close to reality. In the cases here, the application would barely imply safety. Again, it is likely that the strength is overestimated due to the pores not considered in the simulation, since the critical notch stress in the tested samples is higher due to the reduced cross-section compared to the simulation.

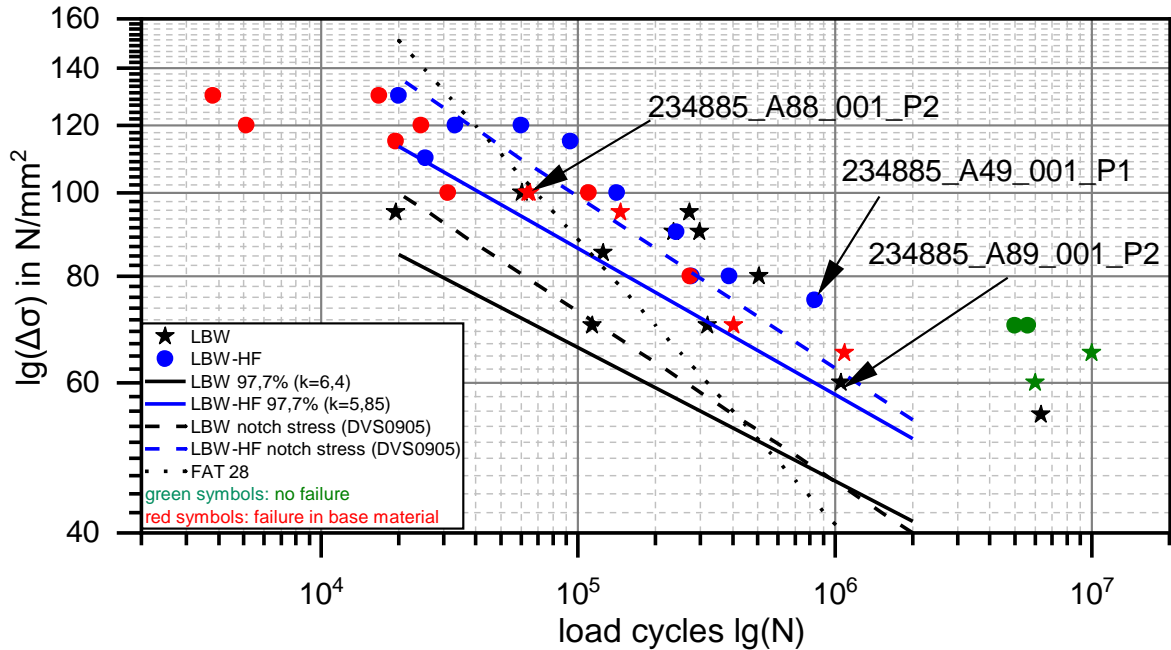


Fig. 8. Results of the fatigue tests of the configuration 3 (butt weld, 3 mm thickness, AlSi9MnMoZr (Batch 2) vs. AlSi9MnMoZr (Batch2))

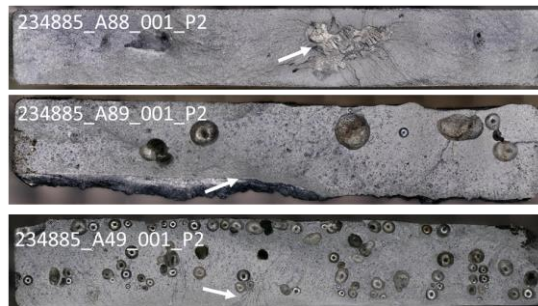


Fig. 9. Fracture surfaces of the fatigue test specimens: 234885_A228_001_P2 (failure in base material); 234885_A49_001_P1 (LBW-HF); 234885_A89_001_P2 (LBW)

3. Summary and conclusion

In the investigations presented here, two laser beam welding processes were used to produce joints in aluminium die castings. High-quality welds could be achieved with both processes. Compared to static laser beam welding, beam oscillation reduced the amount of pores in the welds.

The research question was, whether the normal stress concept according to IIW guideline or the notch stress concept according to DVS guideline is applicable to these welded joints. For this purpose, S-N curves of 3 different material pairings were experimentally determined and the notch stress was estimated by means of FEM after measuring the weld geometry. Generally, all measured values for laser welds in the high cycle fatigue range ($N > 1E6$) exceed the existing regulations for fatigue strength assessment (IIW, FAT). In low cycle fatigue range ($N < 1E5$) the strength of the welds is overestimated.

. At low load cycles, on the other hand, both methods overestimate the strength of the welds. It is assumed

that this is due to the present reduction in cross-sectional area caused by pores and consequently higher nominal and notch stresses. In addition the notch geometry differs especially for the LBW welded specimens in a wide range. Hence, the calculated fatigue strength is depending on the weld seam profile being used. Table 4 summarizes the fatigue strengths determined.

Table 4. Comparison of different fatigue strength (fatigue test, DVS0905, IIW-recommendation, R = 0.1, N = 2E6)

| | Fatigue Test | | DVS0905 | | IIW recommendation |
|------------------------|--------------|--------|---------|--------|--------------------|
| | LBW | LBW-HF | LBW | LBW-HF | LBW + LBW-HF |
| Configuration 1 | 41 | 47 | 47 | 59 | 32,5 |
| Configuration 2 | 49 | 50 | 53 | 48 | 32,5 |
| Configuration 3 | 41 | 52 | 40 | 54 | 32,5 |

Outlook

The results shown here represent an interim status. Currently, further welded joints produced by electron beam and gas metal arc welding are being tested and the occurrence of pores in the weld seams of all welding processes (laser, electron beam and GMAW) is being determined. These results will be published in an appropriate format as soon as possible.

Acknowledgement

This project was funded by Förderung der Industriellen Gemeinschaftsforschung (IGF Vorhaben-Nr.: 20628 BG). On behalf of the authors, we would like to thank the funding body and the project partners of Institute of Joining and Welding (ifs), TU Braunschweig.

References

- Audi AG: audi-technology-portal. URL: <https://www.audi-mediacyber.com/de/audi-a8-50> (Date : 04th may 2021)
- Börner, S.; Dittrich, D.; Mohlau, P.; Leyens, C.; García-Moreno, F.; Kamm, P. H.; Neu, T. R.; Schlepütz, C. M.: In situ observation with x-ray for tentative exploration of laser beam welding processes for aluminium-based alloys. In: Journal of Laser Applications 33 (2021) 1, S. 12026.
- Dittrich, D.; Schulz, S. (2019): Möglichkeit und Perspektiven für das Verbindungsschweißen von Druckgussbauteilen. In: Giesserei : die Zeitschrift für Technik, Innovation und Management (2019) 3, S. 36–41.
ex XIII-2460-13/XV-1440-13; Springer International Publishing AG Switzerland
- Hobbacher A.F. (2016): Recommendations for Fatigue Design of Welded Joints and Components; IIW document IIW-2259-15
- Merkblatt DVS 0905: Industrielle Anwendung des Kerbspannungskonzeptes für den Ermüdungsfestigkeitsnachweis von Schweißverbindungen; DVS Media GmbH , Düsseldorf (2017)
- Teichmann, F.; Pries, H.; Müller, S.; Dilger, K. (2017): Schlussbericht IGF-Vorhaben 18.156 N (ReduPore): Reduzierung der Porenbildung beim Laserstrahlschweißen von Aluminium- Druckgusslegierungen durch reduzierten Umgebungsdruck und/oder Doppelfokustechnik. Braunschweig 2017.
- Winkler, R. (2004): Porenbildung beim Laserstrahlschweißen von Aluminium-Druckguss, Dissertation. Stuttgart 2004.